

Desarrollo, validación y aplicación de un módulo CFD-BEM de aerogeneradores y su interacción con el viento
Dr. Ing. Gabriel Usera
Universidad de la República - Uruguay

1

caffa3d.MBRi : desarrollo de largo plazo, de código abierto

2004 ... 2008
 A Parallel Block-Structured Finite Volume Method for Flows in Complex Geometry with Sliding Interfaces
 Authors: S. Usera, A. Invernizzi, C.A. Ferrás

2014
 A general purpose parallel block structured open source incompressible flow solver
 Authors: Mariana Mendina, Martín Draper, José Paula Ferns Soares, Gabriel Navarro, Gabriel Usera

2015
 Accuracy and reproducibility of patient-specific hemodynamic models of stented intracranial aneurysms: report on the Virtual Intracranial Stenting Challenge 2011.
 Cito S¹, Genta A¹, Arvin M¹, Patro V¹, Palotta J¹, Vermet A¹, Blasco J¹, San Román L¹, Fu W¹, Qian Z¹, Jorga G¹, Minkov O¹, Mendiola F¹, Franco A¹

2017
 Coupled discrete element and finite volume methods for simulating loaded elastic fishnets in interaction with fluid
 Paolo Sassi, Jorge Freire, Paula La Paz, Mariana Mendina, Martín Draper, Gabriel Usera

2018
 Blind test comparison on the wake behind a yawed wind turbine
 Franz Mühlle¹, Jarnik Schotter², Jan Bartl³, Romain Futrzynski⁴, Steve Evans⁵, Luca Bernini⁶, Paolo Schito⁷, Martin Draper⁸, Andrés Gugger⁹, Elektra Kleusberg¹⁰, Michael Hölling¹¹, Joachim Peinke¹², Muyiwa S. Adaramola¹³, and La

2018
 A Large Eddy Simulation-Actuator Line Model framework to simulate a scaled wind energy facility and its application
 Martín Draper¹, Andrés Gugger², Mariana Mendina³, Gabriel Usera⁴, Filippo Carragnolo⁵

Aplicar Tesis Paper Nueva Capacidad

2

caffa3d.MBRi: solver de flujos 3D en volúmenes finitos

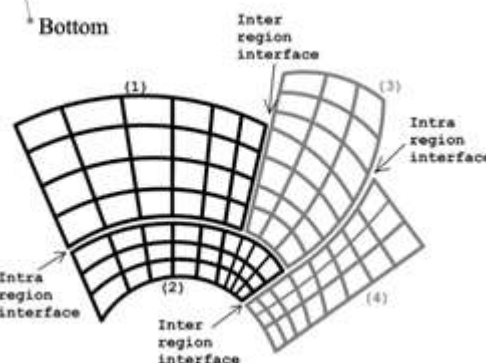
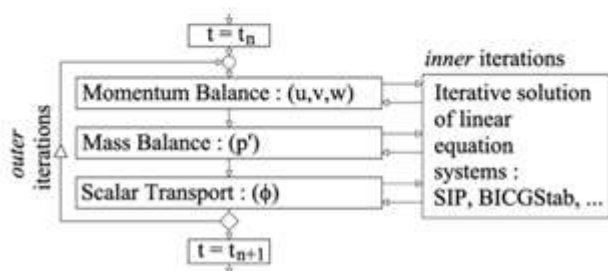
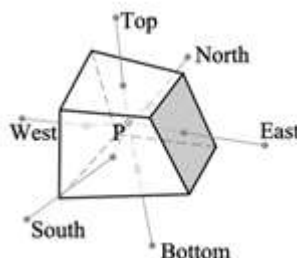


$$\int_S (\mathbf{v} \cdot \hat{\mathbf{n}}_S) dS = 0$$

$$\int_\Omega \rho \frac{\partial u}{\partial t} d\Omega + \int_S \rho u (\mathbf{v} \cdot \hat{\mathbf{n}}_S) dS =$$

$$\int_\Omega \rho \beta (T - T_{ref}) \mathbf{g} \cdot \hat{\mathbf{e}}_1 d\Omega + \int_S -p \hat{\mathbf{n}}_S \cdot \hat{\mathbf{e}}_1 dS +$$

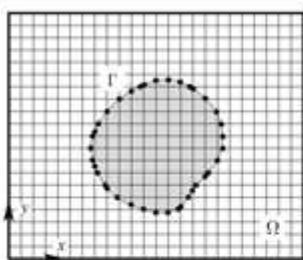
$$\int_S (2\mu \mathbf{D} \cdot \hat{\mathbf{n}}_S) \cdot \hat{\mathbf{e}}_1 dS$$



(Mendina et al, 2014)

3

Condiciones de borde inmersas



$$\int_\Omega \rho \frac{\partial \vec{v}}{\partial t} d\Omega + \int_S \rho \vec{v} (\vec{v} \cdot \hat{\mathbf{n}}_S) dS = \int_\Omega \rho \beta (T - T_{ref}) \vec{\mathbf{g}} d\Omega$$

$$+ \int_S -p \hat{\mathbf{n}}_S dS + \int_S (2\mu \mathbf{D} \cdot \hat{\mathbf{n}}_S) dS + \mathbf{F}_{imb}$$

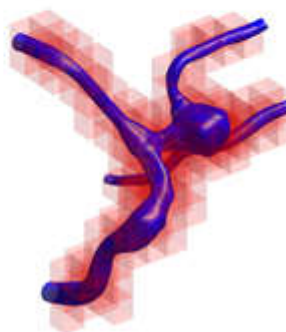
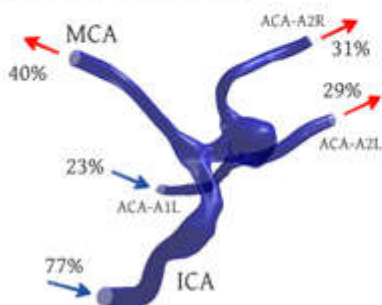


Fig. 14 Patient specific aneurysm geometry with specified flow distribution at inlets and outlets.

(Mendina et al, 2014)

4

Condiciones de borde inmersas

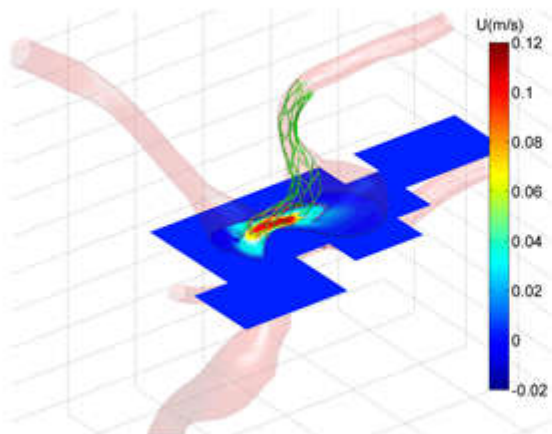


Fig. 16 Detail of flow interaction with stents.

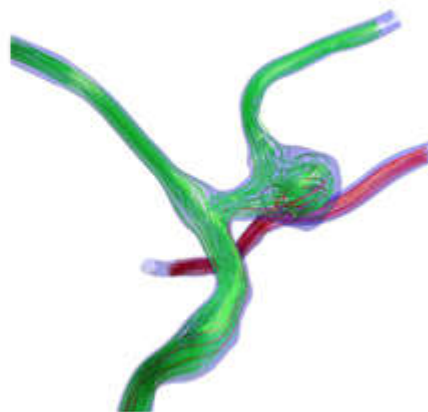


Fig. 18 Streamlines for flow coming from ICA and ACA-A1 arteries. A complex flow pattern with recirculation can be seen inside the aneurysm cavity

5

Dinámica de múltiples cuerpos (multibody dynamics)

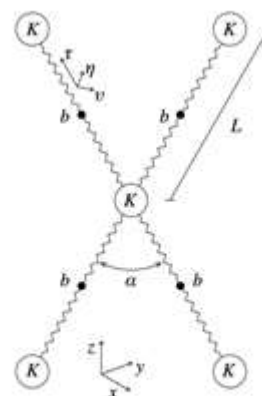
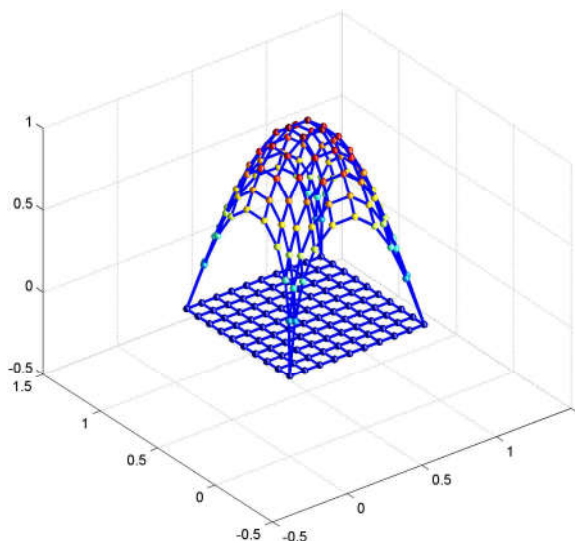


Figure 1: Sketch of the point masses and massless strings.

(Sassi et al, 2017)

6

Dinámica de múltiples cuerpos (multibody dynamics)

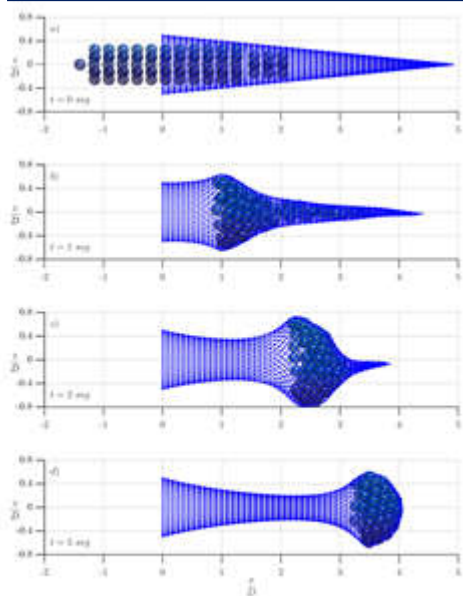


Figure 3: Evolution of the fishnet shape, at time steps $t = 0, 1.0, 2.0, 5.0$ s, as the load is dragged into the fishnet.

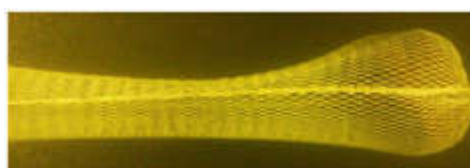
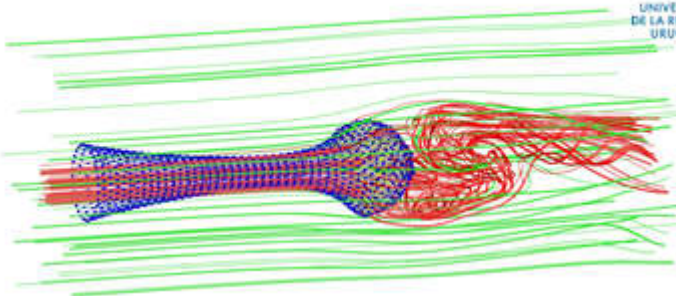
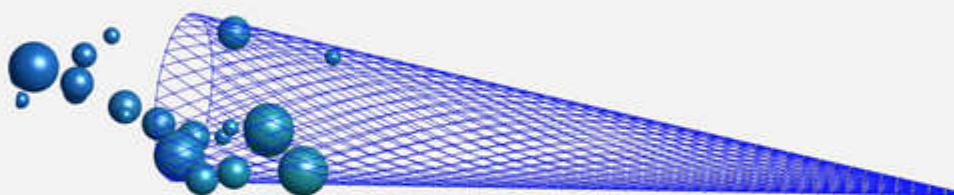


Fig. 5: Shape of the fishnet during the towing tank test.

(Sassi et al, 2017)

7

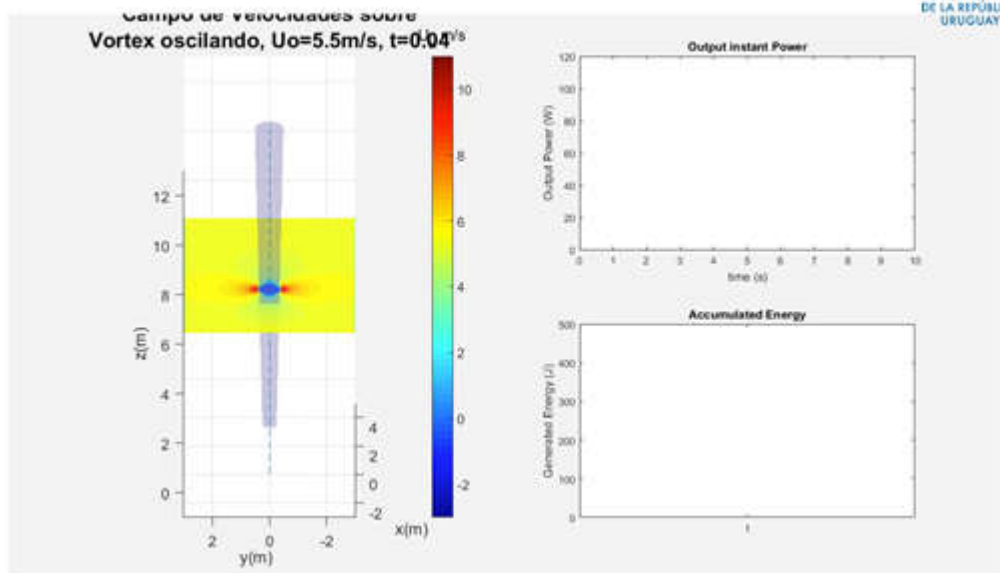
Dinámica de múltiples cuerpos (multibody dynamics)



(Sassi et al, 2017)

8

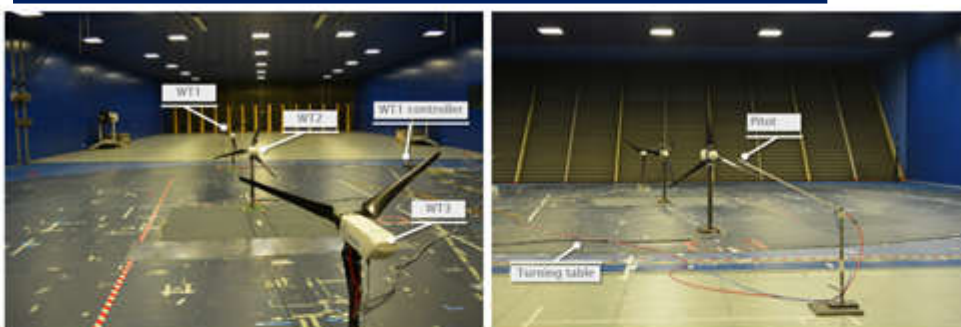
VortexBladeless : turbina sin aspas



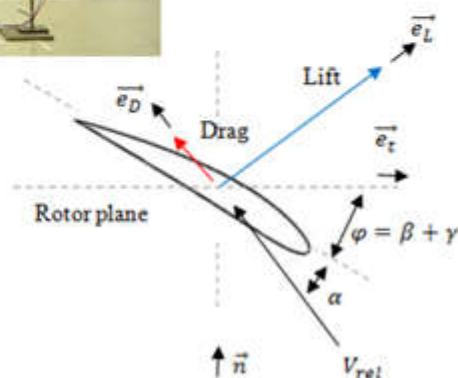
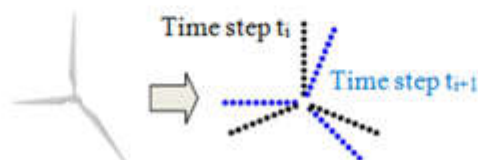
(Sassi et al, 2018)

9

CFD-BEM en modelos a escala de turbinas eólicas

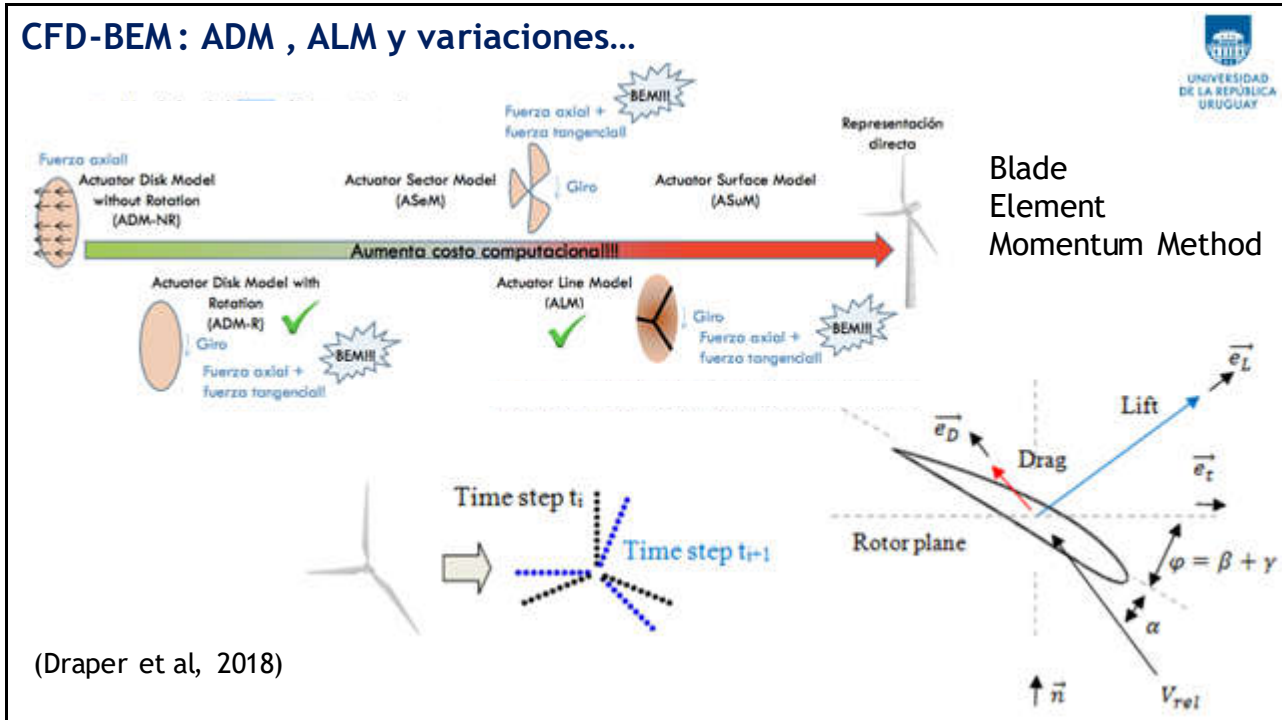


Blade
Element
Momentum Method

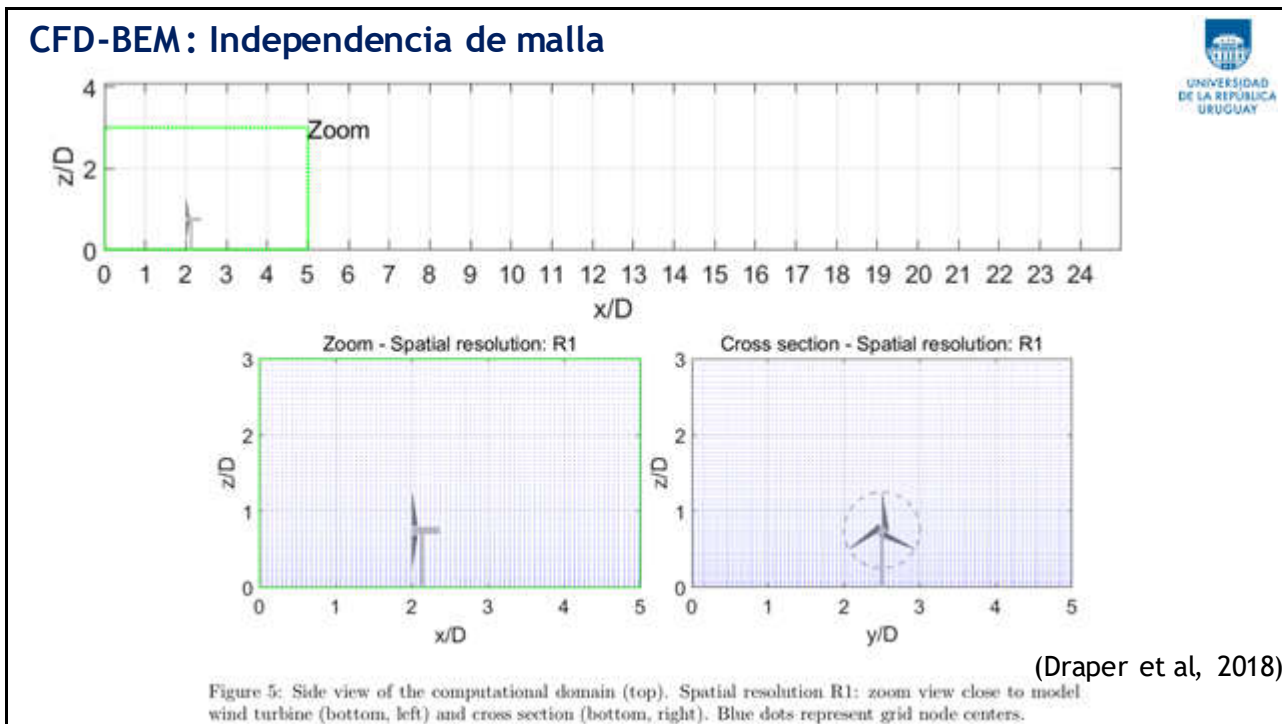


(Draper et al, 2018
with TUM Munich)

10



11



12

CFD-BEM: Independencia de malla



Spatial resolution	N_x	N_y	N_z	$\Delta x(m)$	$\Delta y(m)$	$z_{min}(m)$	$R/\Delta x$	$R/\Delta y$	Nz_{Rotor}
R0	256	64	64	0.107	0.086	0.035	5.1	6.4	22
R1	384	96	80	0.072	0.057	0.022	7.7	9.6	30
R2	512	128	108	0.054	0.043	0.016	10.2	12.8	40

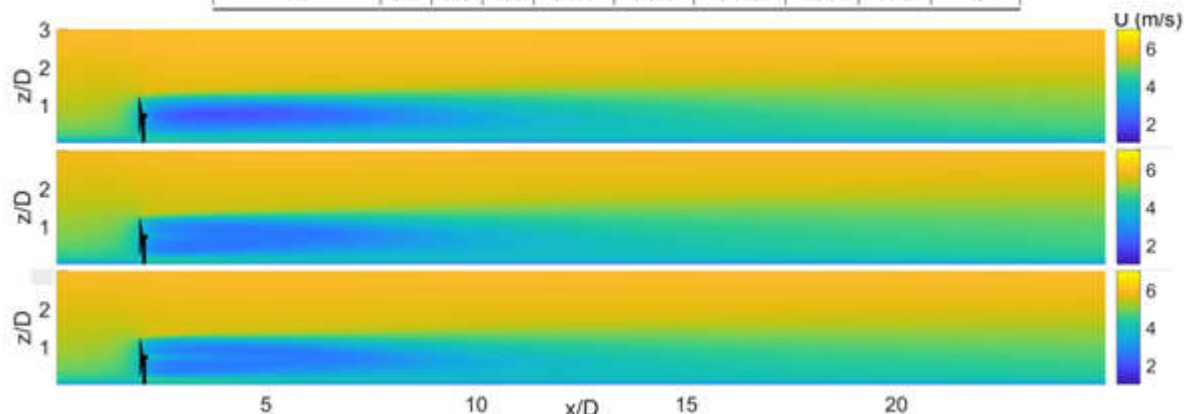
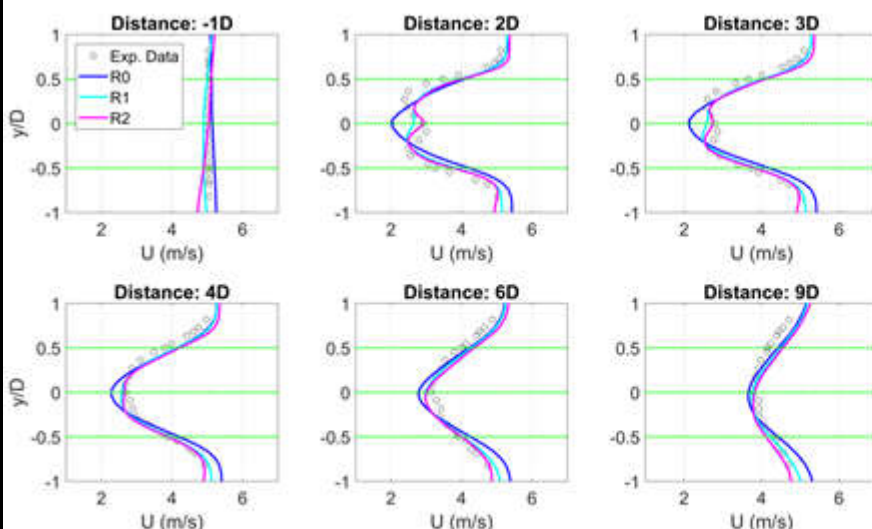


Figure 6: Mean streamwise velocity component in a plane passing through the rotor center. Top: spatial resolution R0, center: spatial resolution R1, bottom: spatial resolution R2. The model wind turbine is sketched in black.

13

CFD-BEM: Independencia de malla



	C_p	C_t
Exp. Data	0.453	0.788
Sim.	R0 0.451 (-0.3%)	0.717 (-9.0%)
	R1 0.428 (-5.4%)	0.716 (-9.2%)
	R2 0.414 (-8.5%)	0.699 (-11.3%)

Figure 7: Mean streamwise velocity component at different locations in the wake at hub height, for the three spatial resolutions considered. Dotted green lines represent the rotor center and blade tips. Open circles represent experimental data.

14

CFD-BEM: Control de estelas por yawing

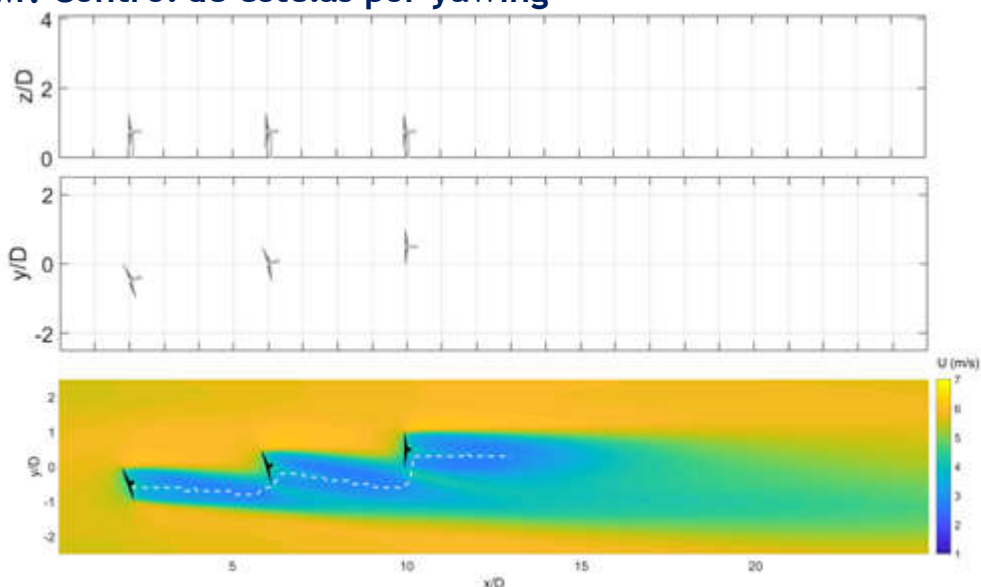


Figure 11: Mean streamwise velocity component in a horizontal plane passing 0.10 m above the rotor center. Spatial resolution R1. The model wind turbines are sketched in black. The white dash line represents the wake center computed from the experimental data by minimization of Equation 7.

15

CFD-BEM: Control de estelas por yawing

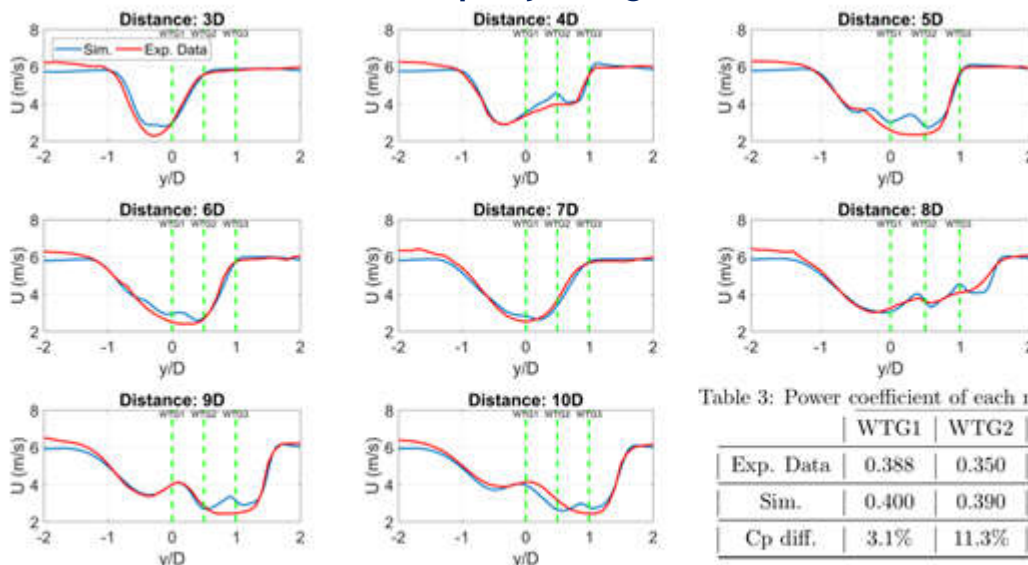


Table 3: Power coefficient of each model wind turbine.

	WTG1	WTG2	WTG3	Total
Exp. Data	0.388	0.350	0.404	1.142
Sim.	0.400	0.390	0.462	1.251
Cp diff.	3.1%	11.3%	14.4%	9.6%

Figure 12: Mean streamwise velocity component in a horizontal plane 0.10 m above the rotor center at different locations in the wake. Spatial resolution R1. The wind turbine rotor centers are represented with green dashed lines. Distance is measured from the rotor plane of the upwind model wind turbine.

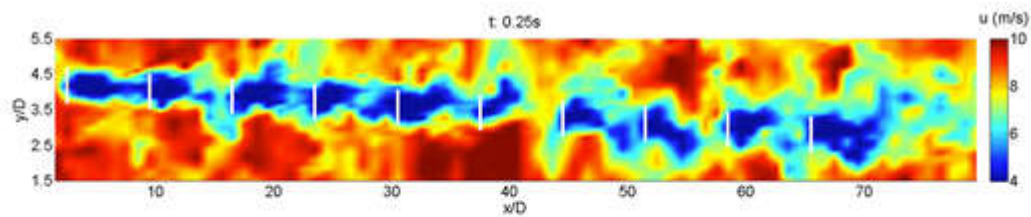
16

CFD-BEM: Horns Rev -> 80 x Vestas V80 2.0 MW



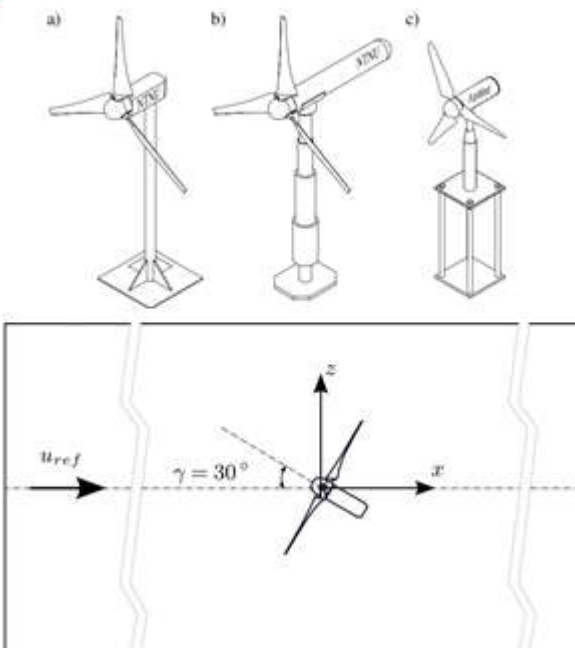
17

CFD-BEM: Horns Rev -> 80 x Vestas V80 2.0 MW



18

CFD-BEM: Blind Test #5 - 2017



(Mühle et al. 2018)

19

CFD-BEM: Blind Test #5 - 2017

Table 2. Overview of simulation methods and parameters. Abbreviations: Improved Delayed Detached Eddy Simulation (IDDES), Large Eddy Simulation (LES), Actuator Line (ACL), Fully Resolved (FR).

Participant	Simulation code	Flow solver type	Rotor model	Airfoil polars	Tower, nacelle	Mesh properties	Number of cells
Siemens	Star-CCM+	IDDES	FR	-	FR	Hexah/polyh.	$\approx 30.0 \cdot 10^6$
POLIMI	ALEVM	LES	ACL	X-Foil	No	Cartesian	$\approx 4.1 \cdot 10^6$
UdelaR	caffa3d	LES	ACL	X-Foil	Yes	Cartesian	$\approx 0.7 \cdot 10^6$
KTH	Nek5000	LES	ACL	Experiments	Yes	Uniform	$\approx 0.08 \cdot 10^6$



BUSINESS NEWS | 11/07/17 24, 2017 | 8:00 PM | 2 YEARS AGO

Siemens to buy CD-adapco for close to \$1 billion: source

Liana B. Baker

3 MIN READ

(Reuters) - Siemens AG (SIEGn.DE), Europe's biggest industrial group, has agreed to buy CD-adapco, a privately held U.S. engineering software firm, for close to \$1 billion in cash, according to a person familiar with the matter.



(Mühle et al. 2018)

20

CFD-BEM: Blind Test #5 - 2017

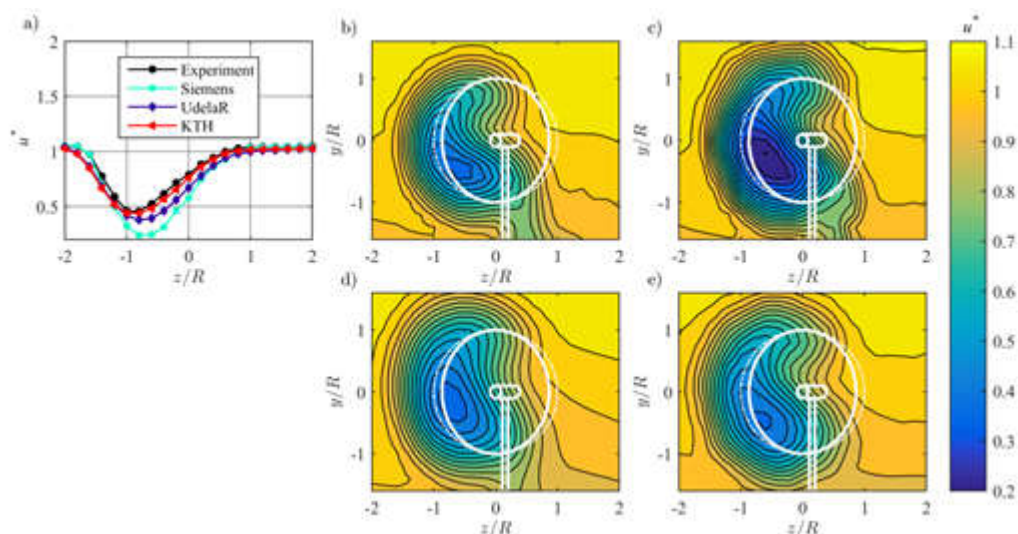


Figure 13. (a) Line plots and (b-e) contour plots for normalized streamwise mean velocity u^* in the wake $3D$ behind upstream ForWind turbine, from (b) experiments, (c) Siemens, (d) UdelaR and (e) KTH and. The white lines represent the turbine rotor, nacelle and tower, solid lines $\gamma = 30^\circ$, dashed lines $\gamma = 0^\circ$.

21

CFD-BEM: Blind Test #5 - 2017



Table 6. Comparison parameters: Skew angle (ξ), wake deflection (δ) and available power in the wake (P^*_{wake}) and their differences to the measurements. Statistical performance measures: $NMSE$ and r for u^* , v^* and k^* at $3D$ and $6D$ behind upstream ForWind turbine.

Institution	Skew angle	Deflection (z/R)	Difference (z/R)	P^*_{wake} [-]	Difference [%]	$NMSE_u$	r_u	r_v	$NMSE_k$	r_k
3D										
Experiments	4.10°	-0.429		0.285						
Siemens	3.71°	-0.388	0.041	0.141	-49.4%	0.012	0.968	0.813	0.383	0.889
UdelaR	4.88°	-0.510	-0.082	0.207	-27.6%	0.007	0.953	0.802	0.734	0.878
KTH	5.27°	-0.551	-0.122	0.233	-18.%	0.005	0.960	0.851	0.202	0.905
6D										
Experiments	3.80°	-0.796		0.533						
Siemens	3.41°	-0.714	0.082	0.430	-19.3%	0.002	0.960	0.845	0.047	0.961
UdelaR	4.00°	-0.837	-0.041	0.540	1.2%	0.001	0.963	0.799	0.067	0.956
KTH	4.19°	-0.878	-0.082	0.475	-11.0%	0.002	0.950	0.884	0.052	0.947

22

CFD-BEM: 'Libertad' 7.7 MW Onshore Wind Farm (4 x Vestas V100)



Figure 1. Libertad wind farm location (left) and layout (right)

(Guggeri et al, 2018)

23

CFD-BEM: 'Libertad' 7.7 MW Onshore Wind Farm (4 x Vestas V100)

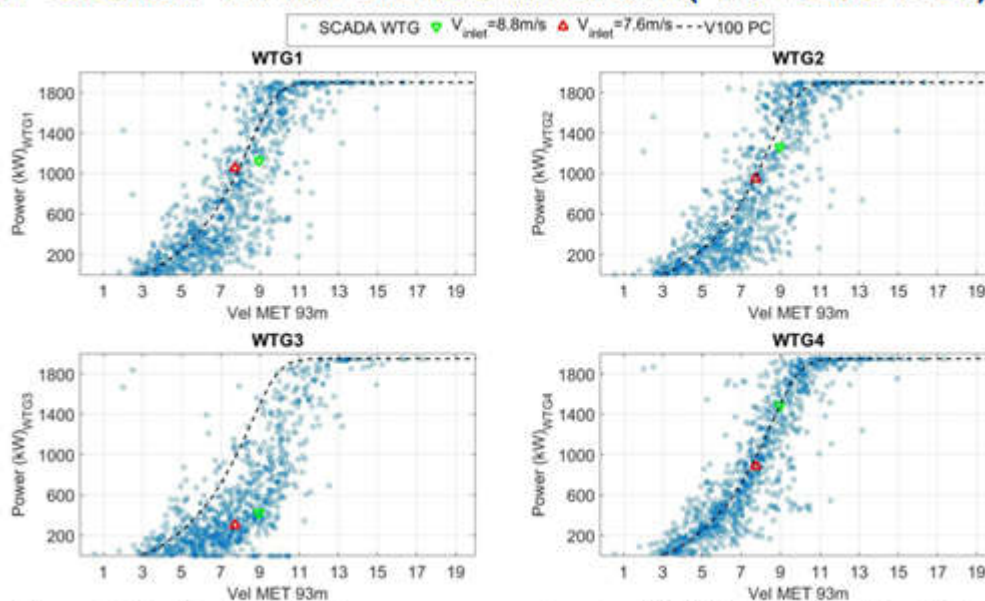


Figure 7. Simulated wind turbines mean power and scattered SCADA data filtered (wind direction $150^\circ \pm 2.5^\circ$), for two inflow conditions.

(Guggeri et al. 2018)

24

Conclusiones



**Modelo CFD-BEM basado en volúmenes finitos,
validado para la simulación de WTG**

**Estructura modular expansible del modelo con
paralelismo masivo basado en MPI**

**Métodos al nivel del estado del arte internacional
en modelado de WTG methods, comparado con
otros grupos de investigación y de la industria.**

25

Próximos pasos



Completar la migración a GPU - CUDA :



CHAMAN

Enfoque de "Rotor Resolved"

Simulaciones aeroelásticas

**... impulsando Spin-Off universitaria de
"nicho" en CFD ...
Buscando socios estratégicos !!**

26



Gracias por su atención.

Gabriel Usera
Profesor Titular - UdelaR
gusera@fing.edu.uy



Red Iberoamericana para el Desarrollo y la Integración de Pequeños Generadores Eólicos (Micro-Eolo)

Conferencias:

FECHA: Jueves 24 de octubre de 2019 **LUGAR:** Edificio 401 - Aula 201